RESEARCH LETTER

Nomogram to help explain probabilistic seismic hazard

John Douglas ⓘ · Laurentiu Danciu ⓘ

Abstract Nomograms are an easy to use and visually attractive graphical tool to solve for any of the variables within an often complex equation. In seismology, the most well-known nomogram is a three-parallel-scale graphic for the calculation of local magnitude given the epicentral distance and trace amplitude. Until the advent of computers, nomograms were often employed by engineers and scientists in many fields as they provide a means for rapid and accurate calculations as well as helping the user understand the sensitivity of the final results to the input parameters. It is this aid to understanding that remains a key attraction of these graphical tools, which are now rarely seen (although they remain common in some fields of medicine where they are used for rapid screening and estimating risks). In this research letter, we present a nomogram summarising the results of simple probabilistic seismic hazard assessments (PSHAs) for peak ground acceleration and elastic response spectral acceleration for a structural period of 1 s and return periods from 100 to 2500 years, where the effects of the activity rate and the slope of the Gutenberg-Richter relation are captured. We believe that this nomogram has considerable educational benefit for engineering seismology students, decision makers and other non-expert users of results of PSHAs.

Keywords Seismic hazard · Earthquake · Probabilistic seismic hazard assessment · Nomogram · Educational

J. Douglas (✉)
Department of Civil and Environmental Engineering, University of Strathclyde, James Weir Building, 75 Montrose Street, Glasgow, G1 1XJ, UK
e-mail: john.douglas@strath.ac.uk

L. Danciu
Swiss Seismological Service, ETH Zurich, Sonneggstrasse 5, Zurich, 8092, Switzerland

1 Introduction

Nomograms (also called nomographs) are graphical tools that provide the user with an analogue computer to evaluate an often complex equation (or group of connected equations) only by means of a paper copy of the nomogram and a straight edge. In seismology, a commonly seen nomogram is one for the calculation of local magnitude given the epicentral distance and the trace amplitude (Richter 1958), although nomograms for other aspects of seismology have been published, e.g. Mahdyiar (1987) presented a nomogram connecting variables of the Brune (1970, 1971) source spectrum. Until the advent of cheap, easy and ubiquitous computing, nomograms were commonly used in many branches of science and engineering to obtain answers easily, quickly and relatively precisely (e.g. Levens 1959). In the current age of spreadsheets and specialist software, nomograms are no longer commonly used by practicing scientists and engineers.

However, they remain a useful educational tool to understand visually the connections among the variables within an equation and the sensitivity of the results to changes in those variables. Nomograms may help those people who prefer pictures to equations understand the inputs and results of complex calculations. This advantage is one reason why nomograms are currently used in medicine when rapidly assessing health risks (e.g. Kattan and Marasco 2010). Another advantage of nomograms is that they cannot be evaluated for combinations of input variables outside the limits of applicability of the equation(s).

In this research letter, we present a nomogram displaying the results of relatively simple probabilistic seismic hazard assessments (PSHAs). In Section 2, the calculations used to construct this nomogram are described and in Section 3 the final nomogram is presented and some example calculations shown using these graphical tools. The results of these calculations are compared to those obtained using the 2013 European Seismic Hazard Model (ESHM13, Woessner et al. (2015)) and the 2014 Earthquake Model of the Middle East (EMME, Giardini et al. (2018)). The article ends with some brief conclusions. The nomogram presented here should not be seen as a replacement for a real PSHA but only as an educational tool.

2 Method for the construction of the nomogram

The aim of any PSHA is to estimate the probabilities of exceeding, within a fixed observational time (e.g. 50 years), different ground-motion levels at a site of interest. The exceedance probabilities of the ground-motion levels are controlled by both the ground-motion model and the forecasts of earthquakes of different magnitudes at various locations (as described by a seismogenic source model).

2.1 Simple probabilistic seismic hazard assessments

To generate our nomogram, we combine the ground-motion model of the ESHM13 (Delavaud et al. 2012) and an area source zone of $2° \times 2°$ (surface area of 49, 560 km^2) and calculate the seismic hazard at the centre of this zone. A time-independent model of seismic activity rates is assumed and defined by an exponential magnitude distribution (Gutenberg and Richter 1944): $\log_{10} N(M) = a - bM$, where $N(M)$ is the cumulative number of earthquakes per unit time equal to or larger than magnitude M, and a and b are empirical constants. The activity rate (a value) represents the total seismic productivity of a given source ($= \log_{10} N(M = 0)$, i.e. log of the number of earthquakes with $M > 0$), and the b value is the negative slope of the recurrence curve expressing average ratio of exponentially distributed small and large earthquakes. This parameter controls the occurrence rates of moderate to large earthquakes. For this nomogram, the range of activity rates is selected to be representative of low to high seismicity areas in the ESHM13 (Woessner et al. 2015). We consider three b values: 0.75, 1.00 and 1.25, to capture the variability in this parameter within ESHM13. An upper bound magnitude of 8.5 has been imposed. The seismicity is concentrated at a depth of 5 km so the nomogram is
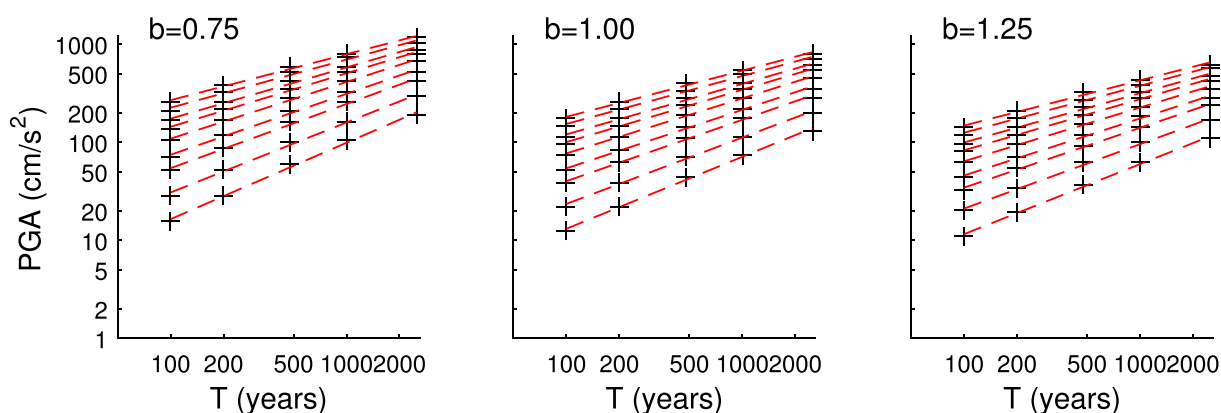
Fig. 1 Fit between the expected PGA computed from PSHA for the nine considered activity rates and three considered b values (crosses) and the power laws fit using Eq. 1 (red dashed lines)
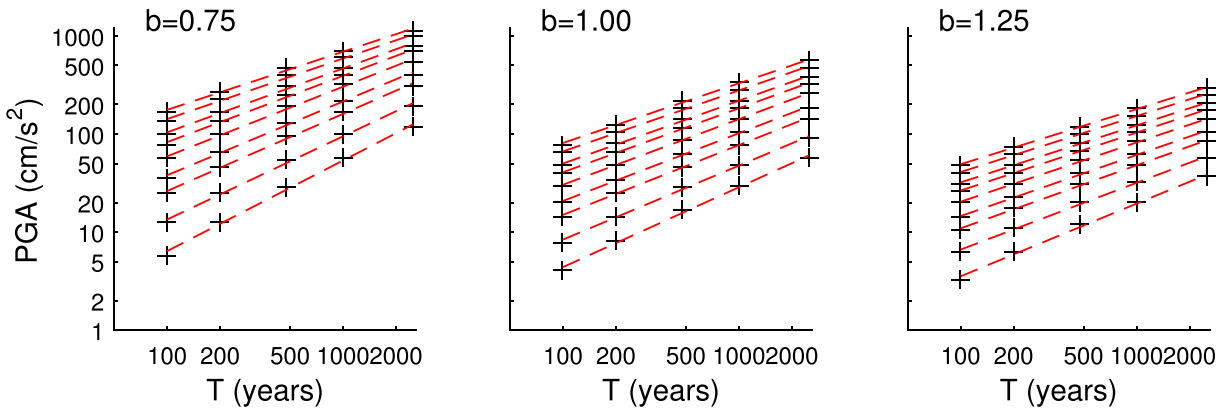
Fig. 2 Fit between the expected SA(1s) computed from PSHA for the nine considered activity rates and three considered *b* values (crosses) and the power laws fit using Eq. 1 (red dashed lines)

only for shallow crustal seismicity. The annual cumulative rates of $(M > M_0)$ considered are 0.05, 0.1, 0.2, 0.3, 0.5, 0.75, 1.0, 1.5 and 2.0 for $M_0 = 4.5$. Hence, the nomogram should not be used outside the range $N(M_0 = 4.5) = 0.05$ to 2.0.

Two ground-motion intensity measures (IMs) are considered: peak ground acceleration (PGA) and pseudo-spectral acceleration for a structural period of 1 s and 5% of critical damping [SA(1 s)]. We consider five mean return periods: 100, 200, 475, 1000, 2500 years, roughly corresponding to the requirements of modern seismic design codes (e.g. Eurocode 8 (Comité Européen de Normalisation 2005)). Hence, the nomogram should not be used outside the range of return periods 100 to 2500 years. The calculations were performed in OpenQuake (Pagani et al. 2014) using extended ruptures.

2.2 Fitting the assessed seismic hazard
with closed-form equations

The results from each of the calculations (where each calculation consists of the same input except for the activity rate) were fit using a power law connecting the PGA or SA(1 s) to the return period. The equation (in terms of natural logarithms to make the relation linear) fit was

$$\ln y = c_0 + c_1 \ln T \qquad (1)$$

where y is PGA or SA(1s) in cm/s^2, T is the return period in years, and c_0 and c_1 are coefficients found by linear least squares regression. The match between

the calculated expected PGAs and SA(1 s) and the predictions using these equations is very close for all cases (Figs. 1 and 2). Power laws modelling the annual frequencies of exceedance of different levels of ground-motion intensity are commonly used to parameterise hazard curves (e.g. Comité Européen de Normalisation 2005; Lubkowski 2010; Kennedy 2011).

Next, for both PGA and SA(1 s), cubic equations are found to predict perfectly (coefficient of determination $R^2 = 100\%$) the values of c_0 and c_1 given $\ln N(M_0 = 4.5)$ for each value of b (Figs. 3 and 4). The Electronic Supplement is an Excel spreadsheet to evaluate Eq. 1.

3 The nomogram

The open-source program pynomo[1] was then used to draw a type 10 nomogram after putting Eq. 1 into the form required for this type, i.e.

$$F_1(u) + F_2(v)F_3(w) + F_4(w) = 0 \qquad (2)$$

where $F_1(u) = \ln y$, $F_2(v) = -\ln T$, $F_3(w) = c_1(N)$ and $F_4(w) = -c_0(N)$. The resulting nomogram is shown in Fig. 5. To read Fig. 5, connect two of the variables (e.g. $N(M_0 = 4.5)$ and return period) with a straight line and where it crosses the axis for the third variable that is its value (e.g. PGA). Example
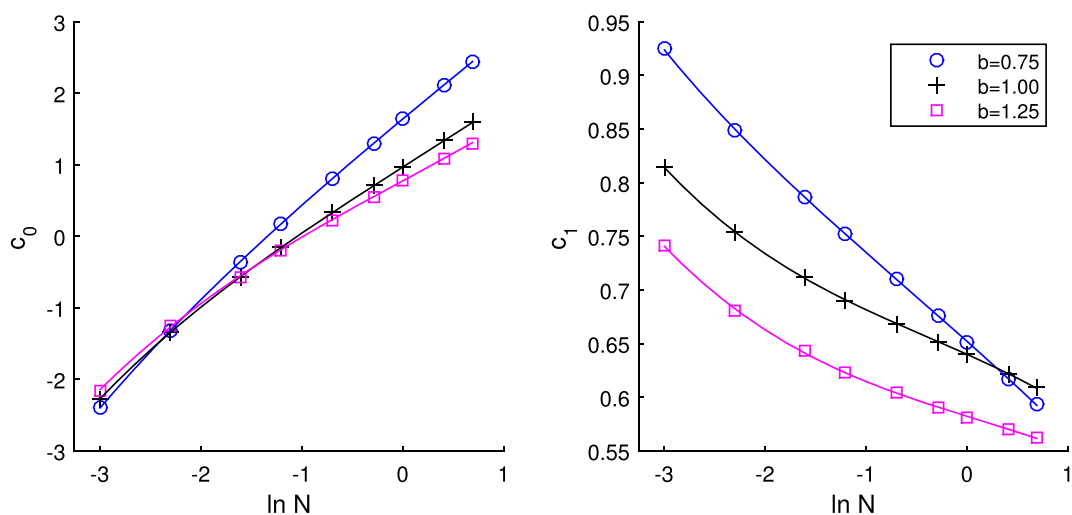
---

[1] http://pynomo.org/wiki/index.php/Main_Page
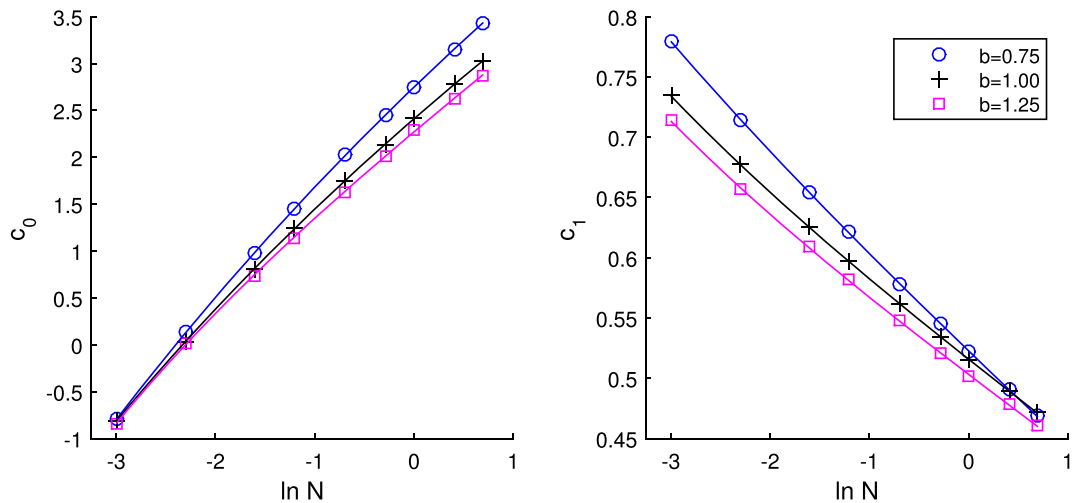
Fig. 3 The relationship between c_0 and c_1, i.e. the coefficients of Eq. 1, and $\ln N(M_0 = 4.5)$, i.e. log of the number of earthquakes of magnitude greater than 4.5, and the fitted cubic equations (for PGA)

calculations are shown using red lines for a return period of 475 years and an activity rate of $N(M_0 = 4.5) = 0.1$ (a moderate seismicity zone).

Needless to say that the comparison between estimates from the simplified nomogram and those from a real PSHA (e.g. ESHM13) is challenging for two main reasons. Firstly, the latter is a full hazard calculation that blends full distributions of the inputs, in particular the alternative ground-motion and seismogenic source models. Secondly, the hazard calculation with Open-Quake uses extensive ruptures for large magnitudes, which when combined with permissible boundaries of

seismic sources can result in a more complex hazard pattern than the estimates from a single seismic source. In the analysis, we have considered a single seismogenic source and the ground-motion models for two seismo-tectonic domains: the active shallow crust and stable continental region as described in Delavaud et al. (2012). Hence, the contributions of the two ground-motion models are reflected in the hazard results.

The expected PGAs and SA(1 s) for sites covered by ESHM13 are obtained for the five return periods from the European Facilities of Earthquake Hazard

Fig. 4 The relationship between c_0 and c_1, i.e. the coefficients of Eq. 1, and $\ln N(M_0 = 4.5)$, i.e. log of the number of earthquakes of magnitude greater than 4.5, and the fitted cubic equations (for SA(1 s))
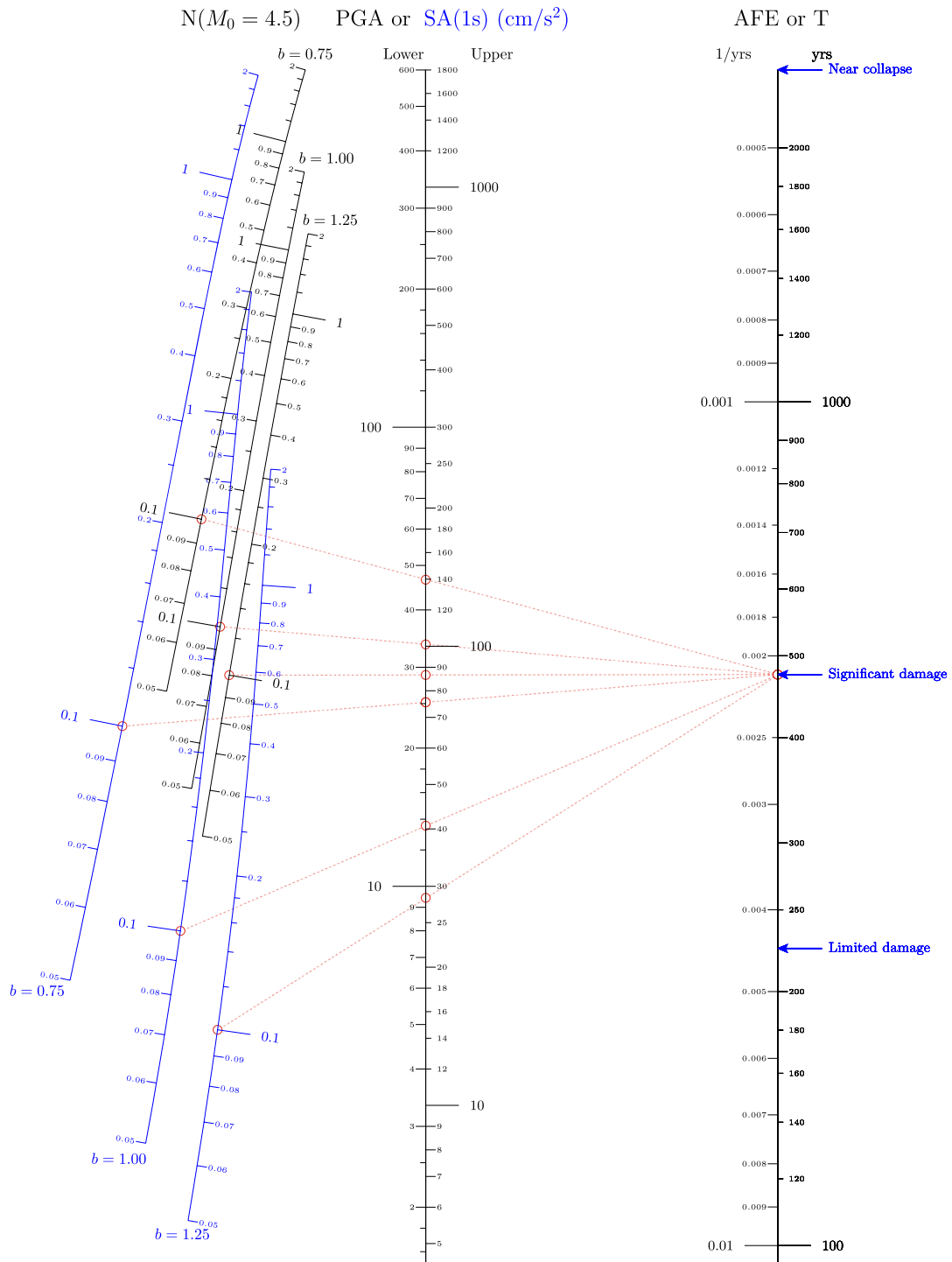
Fig. 5 Nomogram for the assessed seismic hazard in terms of PGA and SA(1 s). The axes at the left hand side (indicating $N(M_0 = 4.5)$), i.e. the number of earthquakes larger than or equal to magnitude 4.5 within a $2 \times 2°$ square centred on the location of interest) are for PGA (black) and SA(1 s) (blue). AFE means annual frequency of exceedance and T means return period. The arrows on the right-hand side indicate the return periods corresponding to the three structural performance requirements defined by Eurocode 8 (Comité Européen de Normalisation 2005). The red dashed lines indicate some example calculations made using the nomogram

Table 1 Comparison between the expected PGAs and SA(1 s)s for return periods of 225 and 2475 years obtained using the nomogram and from ESHM13 for 14 European capital cities

IM		PGA (cm/s^2)				SA(1 s) (cm/s^2)			
T (yr)		225		2475		225		2475	
City	N	Nomogram	ESHM13	Nomogram	ESHM13	Nomogram	ESHM13	Nomogram	ESHM13
Athens	1.33	213	220	702	648	101	133	457	442
Belgrade	0.45	113	71	442	218	48	32	243	109
Bern	0.24	75	71	327	230	31	34	165	114
Bratislava	0.10	41	65	209	240	16	25	96	99
Brussels	0.02	N/A	40	N/A	137	N/A	20	N/A	77
Bucharest	0.13	49	168	238	407	19	134	112	341
Lisbon	0.47	116	152	452	500	50	63	250	266
Ljubljana	0.74	153	160	552	439	68	64	327	221
Podgorica	1.02	184	171	632	499	85	80	394	297
Reykjavik	1.31	212	312	699	805	100	165	453	605
Rome	1.22	203	128	680	367	96	59	436	205
Sarajevo	0.45	113	81	443	255	48	41	243	129
Tirana	2.65	N/A	281	N/A	715	N/A	142	N/A	492
Zagreb	0.60	135	163	504	477	59	64	289	246

IM means intensity measure, T means return period and N is the average number of earthquakes with $M_w \geq 4.5$ per year within a $2° \times 2°$ box centred on the city in SHEEC (Grünthal et al. 2013). For precision, the values reported in the 'Nomogram' columns were actually evaluated using the Excel spreadsheet provided in the Electronic Supplement. The values in the 'ESHM13' columns were obtained by interpolating the hazard curves for the city from EFEHR in log-log space at the return periods of interest

and Risk (EFEHR).[2] These hazard estimates are then grouped by the seismic activity parameters (the *a* and *b* values discussed in Section 2.1) for the source zone enclosing the selected site. The activity rates were normalised to the surface area of the $2° \times 2°$ area considered for the simple PSHA. It was found that the expected PGAs and SA(1 s) estimated using the nomogram were generally within 50% of those from ESHM13 for locations with the same normalised activity rates. We also conducted a comparison for locations covered by EMME and a similarly close match was found. Therefore, we have chosen to indicate on Fig. 5 the rough limits of the nomogram to provide accurate hazard estimates (as measured by the match to results from ESHM13 and EMME for many locations) by giving a range of ±50% around the exact PGAs and SA(1 s) obtained from the simple PSHAs. For example, the simple PSHA for a return period of 475 years, $N(M_0 = 4.5) = 0.1$ and $b = 1.00$ gives a exact PGA value of 67 cm/s^2 but rather than indicate

this on the central nomogram axis the range from 34 to 101 cm/s^2 (i.e. ± 50% of this exact value) is shown instead.

To compare estimates from the nomogram to those from real PSHAs, hazard results from ESHM13 for some example locations (14 European capitals) are listed in Table 1 alongside estimates obtained from the nomogram, assuming $b = 1.00$ (often a valid assumption (e.g. Frohlich and Davis 1993)). To obtain $N(M_0 = 4.5)$ for each of the considered locations, the instrumental earthquake catalogue used for the ESHM13 (SHEEC 1900-2006, (Grünthal et al. 2013)) was queried for a $2° \times 2°$ box centred on the location to obtain the average number of earthquakes with $M_w \geq 4.5$ per year.

This comparison shows that for eight of the considered cities (Athens, Bern, Bratislava, Lisbon, Ljubljana, Reykjavik, Podgorica and Zagreb) hazard levels from the nomogram are generally within 50% of those from the real PSHA of ESHM13. Such a convergence among results from the simple PSHAs (represented by the nomogram on Fig. 5) and this regional PSHA was

found despite differences between the ground-motion models used in ESHM13 and the complexities of its seismogenic source models. Although it could be surprising that the simple PSHA used to derive the nomogram can provide rough estimates of the results from a real PSHA, it can be partially explained by the observation that hazard disaggregation (Bazzurro and Cornell 1999) often shows that the most important earthquakes are within 100 km (or even closer) from the location of interest (e.g. Barani et al. 2009). Therefore, the assumption that the location is within a single local source zone of uniform seismicity can often be made.

Table 1, however, does demonstrate the limitations of the nomogram. When the average annual number of earthquakes with $M_w \geq 4.5$ is less than 0.05 (e.g. Brussels) or greater than 2.0 (e.g. Tirana), the nomogram cannot be used (because of the lower limit other capital cities in the north of Europe, e.g. London and Oslo, where the seismicity is low are not included in this table). When the seismic hazard is dominated by distant earthquakes (e.g. Bucharest, for which the Vrancea earthquake zone is important), the nomogram significantly underestimates the results of the real PSHA. In contrast, if the location is close to but not within an area of high seismicity (e.g. Belgrade, Rome and Sarajevo), the nomogram can overestimate the results from a real PSHA. It should also be noted that if the local seismicity means that b does not equal unity then the difference between the nomogram and the results of a real PSHA could be large.

4 Conclusions

In this short research letter, we have presented a nomogram (Fig. 5) to capture the results of a series of simple probabilistic seismic hazard assessments (PSHAs) for return periods between 100 and 2500 years and peak ground acceleration and pseudo-spectral acceleration for a structural period of 1 s and 5% of critical damping. The characteristics of the seismicity modelled are the annual average number of earthquakes of $M_w \geq 4.5$ within a $2° \times 2°$ square centred on the site of interest and the slope of the Gutenberg-Richter earthquake recurrence relation. The purpose of this nomogram is not to replace real PSHAs but to give the user a graphical understanding of the influence of the different inputs to PSHAs. For example, the nomogram shows the relatively minor influence of the b value

on peak ground acceleration but a large influence for long-period spectral accelerations. It also shows that the expected ground motions for a given return period increase as the activity rate increases but that the rate of increase reduces. In conclusion, we contend that this nomogram provides the non-expert with valuable insights into PSHAs that is not possible with standard means of presentation.

References

Barani S, Spallarossa D, Bazzurro P (2009) Disaggregation of probabilistic ground-motion hazard in Italy. Bulletin of the Seismological Society of America 99(5):2638–2661. https://doi.org/10.1785/0120080348

Bazzurro P, Cornell CA (1999) Disaggregation of seismic hazard. Bulletin of the Seismological Society of America 89(2):501–520

Brune JN (1970) Tectonic stress and the spectra of seismic shear waves from earthquakes. J Geophys Res 75(26):4997–5009

Brune JN (1971) Correction. J Geophys Res 76(20):5002

Comité Européen de Normalisation (2005) Eurocode 8, Design of structures for earthquake resistance — Part 1: General rules, seismic actions and rules for buildings. European Standard NF EN 1998–1

Delavaud E, Cotton F, Akkar S, Scherbaum F, Danciu L, Beauval C, Drouet S, Douglas J, Basili R, Sandikkaya MA, Segou M, Faccioli E, Theodoulidis N (2012) Toward a ground-motion logic tree for probabilistic seismic hazard assessments in Europe. J Seismology 16(3):451–473. https://doi.org/10.1007/s10950-012-9281-z

Frohlich C, Davis SD (1993) Teleseismic b values; Or, much ado about 1.0. J Geophys Res 98(B1):631–644

Giardini D, Danciu L, Erdik M, Şeşetyan K, Demircioğlu Tümsa MB, Akkar S, Gülen L, Zare M (2018) Seismic hazard map of the Middle East. Bulletin of Earthquake Engineering 16(8):3567–3570. https://doi.org/10.1007/s10518-0347-3

Grünthal G, Wahlström R, Stromeyer D (2013) The SHARE European Earthquake Catalogue (SHEEC) for the time period 1900–2006 and its comparison to European-Mediterranean Earthquake Catalogue (EMEC). J Seismology 17(4):1339–1344. https://doi.org/10.1007/s10950-013-9379-y

Gutenberg R, Richter CF (1944) Frequency of earthquakes in California. Bulletin of the Seismological Society of America 34(4):185–188

Kattan MW, Marasco J (2010) What is a real nomogram? Seminars in Oncology 37(1):23–26. https://doi.org/10.1053/j.seminoncol.2009.12.003

Kennedy RP (2011) Performance-goal based (risk informed) approach for establishing the SSE site specific response spectrum for future nuclear power plants. Nuclear Engineering and Design 241:648–656. https://doi.org/10.1016/j.nucengdes.2010.08.001

Levens AS (1959) Nomography, 2nd edn. Wiley, New York

Lubkowski ZA (2010) Deriving the seismic action for alternative return periods according to Eurocode 8. In: Proceedings of the 14th European conference on earthquake engineering

Mahdyiar M (1987) A nomograph to calculate source radius and stress drop from corner frequency, shear velocity, and seismic moment. Bulletin of the Seismological Society of America 77(1):264–265

Pagani M, Monelli D, Weatherill G, Danciu L, Crowley H, Silva V, Henshaw P, Butler L, Nastasi M, Panzeri L, Simionato M, Viganò D (2014) OpenQuake Engine: an open hazard (and risk) software for the Global Earthquake Model. Seismological Res Lett 85(3):692–702. https://doi.org/10.1785/0220130087

Richter CF (1958) Elementary seismology. Freeman and Co., San Francisco

Woessner J, Danciu L, Giardini D, Crowley H, Cotton F, Grünthal G, Valensise G, Arvidsson R, Basili R, Demircioglu MB, Hiemer S, Meletti C, Musson RW, Rovida AN, Sesetyan K, Stucchi M, The SHARE Consortium (2015) The 2013 European seismic hazard model: key components and results. Bulletin of Earthquake Engineering 13(12):3553–3596. https://doi.org/10.1007/s10518-015-9795-1